

Shinohara, M., Salisbury, M.H., and Richter, C. (Eds.)  
*Proceedings of the Ocean Drilling Program, Scientific Results Volume 195*

## DATA REPORT: PALEOMAGNETIC AND ENVIRONMENTAL MAGNETIC PROPERTIES OF SEDIMENTS FROM SITE 1202 (KUROSHIO CURRENT)<sup>1</sup>

Alessandra Venuti<sup>2</sup>, Carl Richter<sup>3</sup>, and Kenneth L. Verosub<sup>4</sup>

### ABSTRACT

We present paleomagnetic and mineral magnetic results from ocean sediments from the southern Okinawa Trough (west Pacific). We obtained samples from two holes from Ocean Drilling Program Site 1202 and determined the natural remanent magnetization, magnetic susceptibility, anhysteretic remanent magnetization (ARM), hysteresis properties, and thermomagnetic behavior. Hole 1202A was studied between 100 and 120 meters below seafloor (mbsf) and Hole 1202B between 0 and 140 mbsf, both at 1-cm resolution. Hysteresis properties and thermomagnetic behavior were measured on selected samples. The measurements show a stable magnetization carried by pseudo-single-domain-sized low-titanium magnetite. Magnetic inclinations are predominantly positive and record the Brunhes (C1n) normal polarity chron. Susceptibility and ARM, as well as the environmentally significant rock magnetic ratios ( $ARM/k$  and  $ARM_{30\text{ mT}}/ARM_{0\text{ mT}}$ ), reflect changes in sediment input from Taiwan and the East China Sea continental shelf changes in the path of the Kuroshio Current and changes in climatic conditions.

### INTRODUCTION

The Kuroshio Current is the largest western boundary current in the North Pacific Ocean, and because of its high velocity and thermal ca-

<sup>1</sup>Venuti, A., Richter, C., and Verosub, K.L., 2005. Data report: Paleomagnetic and environmental magnetic properties of sediments from Site 1202 (Kuroshio Current). In Shinohara, M., Salisbury, M.H., and Richter, C. (Eds.), *Proc. ODP, Sci. Results*, 195, 1–14 [Online]. Available from World Wide Web: <[http://www-odp.tamu.edu/publications/195\\_SR/VOLUME/CHAPTERS/111.PDF](http://www-odp.tamu.edu/publications/195_SR/VOLUME/CHAPTERS/111.PDF)>. [Cited YYYY-MM-DD]

<sup>2</sup>Istituto Nazionale di Geofisica e Vulcanologia, Via di Vigna Murata 605, 00143 Roma, Italy. [venuti@ingv.it](mailto:venuti@ingv.it)

<sup>3</sup>Department of Geology, University of Louisiana at Lafayette, PO Box 44530, Lafayette LA 70504, USA.

<sup>4</sup>Department of Geology, University of California at Davis, One Shields Avenue, Davis CA 95616, USA.

Initial receipt: 18 June 2004

Acceptance: 4 January 2005

Web publication: 4 June 2005

Ms 195SR-111

capacity, the current strongly influences east Asian climate, upper-ocean thermal structure, and the distribution of marine sediment in this region (Jian et al., 2000). Presently, after flowing along the eastern side of the island of Taiwan, the current is deflected northeastward into the Okinawa Trough, located between Japan and Taiwan (Fig. F1). This flow, coupled with the enormous input of terrigenous material from the East China shelf and from the island of Taiwan, results in extremely high rates of sedimentation in the southern Okinawa Trough.

However, the path and strength of the Kuroshio Current have changed several times during the late Quaternary, influencing the climate in the northwestern Pacific (Ujiié and Ujiié, 1999). For example, according to Ujiié et al. (1991), during the last glacial maximum (LGM), the current was not present at all in the Okinawa Trough area but was shifted southward at the southern end of the Ryukyu arc, causing cooling in the waters in the trough. Other authors have reached different conclusions about the path of the Kuroshio Current (Sawada and Handa, 1998; Ujiié and Ujiié, 1999; Jian et al., 2000), and its history and evolution are still controversial.

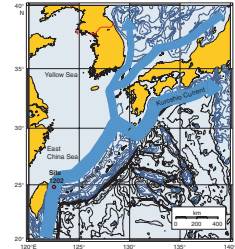
In this report, we present paleomagnetic data from an investigation of sediment cores recovered from Ocean Drilling Program (ODP) Site 1202 in the southern Okinawa Trough. We also present environmental magnetic data of variations in the composition, concentration, and grain-size distribution of the magnetic material in the cores.

## GEOLOGICAL SETTING AND LITHOSTRATIGRAPHY

Site 1202 (24°48.2'N, 122°30.00'E) is located in 1274 m deep water on the southern slope of the southwestern part of the Okinawa Trough, which extends from Kyushu, Japan, to the northeast side of the island of Taiwan (Fig. F1). The Okinawa Trough is an active intracontinental backarc basin bordered to the south by the Ryukyu arc-trench system (Sibuet et al., 1998; Wang et al., 1999). Sedimentation rates are high because of terrigenous input from Taiwan and the East China Sea shelf (Boggs et al., 1979; Lin and Chen, 1983). The East China Sea continental shelf was above sea level during the LGM, and only the Okinawa Trough was submerged. Unlike most parts of the Pacific, the seafloor in the Okinawa Trough lies well above the carbonate compensation depth, so calcareous microfossils can be preserved. This makes Site 1202 an ideal site for obtaining a high-resolution record of the Quaternary history of the Kuroshio Current.

A 20-m-thick sequence from Hole 1202A (100–120 meters below sea floor [mbsf]) that contained a suspected magnetic excursion (Mono Lake; 105–108 mbsf) (Shipboard Scientific Party, 2002) and the entire sequence from Hole 1202B are the subject of this report. Both holes were cored at the end of Leg 195 with the advanced piston corer (APC). Hole 1202B was cored with the APC to refusal at a depth of 111.6 mbsf and was deepened with the extended core barrel (XCB) to 140.5 mbsf. The sedimentary succession consists of one lithostratigraphic unit characterized by homogeneous, slightly calcareous, bioturbated clayey silt with isolated sandy intervals and fine sand laminae. Thin sandy layers have been interpreted to be mostly detrital carbonate, indicating episodes of turbidity current activity (Shipboard Scientific Party, 2002). There are no visible ash layers, but one sample with volcanic glass

F1. Location of Site 1202, p. 8.



particles was identified by smear slide analysis conducted on the Hole 1202D sequence (Shipboard Scientific Party, 2002).

Biostratigraphic analysis (Shipboard Scientific Party, 2002) of core catcher samples, especially the absence of pink *Globigerinoides ruber*, indicates that the sequence is younger than 127 ka, suggesting that the average sedimentation rate is at least 320 cm/k.y. Previous work (Jian et al., 2000) on Holocene sediments from southern Okinawa Trough showed an average sedimentation rate of ~20 cm/k.y. with exceptionally abrupt changes in the sedimentation rates, probably caused by sudden changes in the input of terrigenous material.

## SAMPLING AND METHODS

The working halves of cores from Holes 1202A and 1202B were sampled using U-channels at the ODP Gulf Coast Repository in College Station, Texas. The U-channels were then shipped to the Paleomagnetism Laboratory at the University of California, Davis, where the measurements were made.

Natural remanent magnetization (NRM) and anhysteretic remanent magnetization (ARM) were measured at 1-cm intervals using an automated 2G Enterprises model 755R cryogenic magnetometer (Weeks et al., 1993; Verosub, 1998). Initially the samples were stepwise demagnetized in peak alternating fields (AFs) of 0, 20, 30, 40, 50, and 60 mT, and the NRM was measured after each step. An ARM was then imparted using a peak AF of 100 mT and a direct bias field of 0.05 mT. The samples were then stepwise demagnetized with peak AFs of 0, 10, 20, 30, 40, 50, and 60 mT.

Low-field magnetic susceptibility (MS) was measured every centimeter using a Bartington susceptibility meter and a field surface probe. This process required the U-channels to be opened in order to place the surface probe directly onto the sediment.

The temperature variation of MS (up to a maximum temperature of 700°C) was measured on 13 bulk samples evenly spaced along Hole 1202B using a furnace-equipped Kappabridge KLY-3 at the Istituto Nazionale di Geofisica e Vulcanologia in Rome, following procedures described by Hrouda (1994). Hysteresis parameters were measured at University of California, Davis, using a Princeton Measurements Corporation alternating gradient magnetometer.

## REVISED DEPTH MODEL

Core expansion in recovered deep-sea sediment cores occurs because of pressure release, degassing, and elastic rebound (Moran, 1997). This can lead to core sections overlapping at core breaks and can cause apparently duplicate measurements when using the original mbsf depth scale. We constructed a revised mbsf (rmbsf) scale for Hole 1202B to avoid overlapping measurements by adding a constant offset to each core (Table T1). Conversion between the two depth scales is straightforward and requires addition of the offset constant to the mbsf scale or subtraction from the rmbsf scale.

---

T1. Revised depth model accounts, p. 14.

---

## PALEOMAGNETIC RESULTS

### Hole 1202A

The U-channels were easily demagnetized by AF techniques and exhibited very satisfactory demagnetization behavior. Most of the NRM intensity is removed by peak fields of 50–60 mT, as shown by the intensity decay curves (Fig. F2A). Orthogonal vector component diagrams and stereographic projections reveal only one single component of magnetization. The demagnetization behavior and other magnetic properties (see below) are consistent with magnetite as the primary magnetic carrier. Magnetic parameters including magnetic inclinations and intensity from Hole 1202A are shown in Figure F3. The NRM inclinations are mostly positive and reach their highest values in the intervals between 108 and 112 mbsf and between 117.6 and 118.5 mbsf. The suspected geomagnetic excursion (Shipboard Scientific Party, 2002) could not be confirmed.

### Hole 1202B

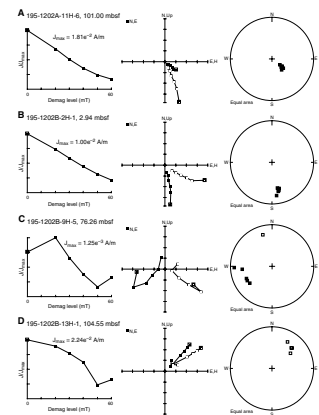
In the upper part of the sequence (0–69.4 rmbfsf), orthogonal vector component diagrams of the NRM again exhibit very satisfactory demagnetization behavior (Fig. F2B). A secondary NRM component, imprinted by the coring or sampling process, is removed after the 20-mT demagnetization step, and the characteristic remanent magnetization (ChRM) can be readily determined. In the interval from 69.4 to 86.5 rmbfsf, the NRM has a relatively low intensity (Fig. F4) that is unstable during demagnetization. Both broad directional variations and remagnetizations at higher demagnetization steps have been observed in this interval (Fig. F2C). In the remainder of the section, the NRM usually demagnetizes well up to peak fields of 50 or 60 mT, but some remagnetization occurs in higher fields (Fig. F2D). Similar behavior has been observed at other locations (e.g., Shipboard Scientific Party, 2001) and may provide evidence for the presence of iron sulfides, which can acquire a gyromagnetic remanence during the AF demagnetization (Snowball, 1997; Sagnotti and Winkler, 1999). We cannot exclude the possibility that the remagnetization is caused by a spurious component during the demagnetization process.

The magnetic parameters from Hole 1202B are shown in Figure F4. The NRM inclinations are mostly positive, but shallow and negative values occur in intervals 50–62, 73–81, and 103–110 rmbfsf. The NRM inclinations are distinctly noisier below 114 rmbfsf, which is the depth at which the coring system was changed from APC to XCB.

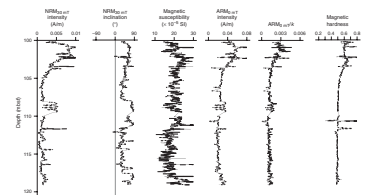
The geomagnetic field at the latitude of Site 1202 (24.8°N) has an inclination of 42.7°, assuming a geocentric axial dipole model that is sufficiently steep to determine magnetic polarity in the APC and XCB cores, which lack azimuthal orientation.

Positive magnetic inclinations indicate that only the Brunhes (C1n) normal polarity chron (Berggren et al., 1995) is recorded in these sediments. Whether the Brunhes Chron is complete cannot be determined from the magnetostratigraphy.

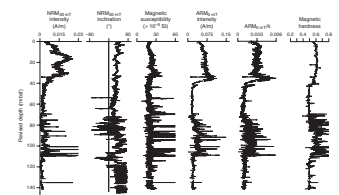
F2. AF demagnetization behavior, p. 9.



F3. Hole 1202A magnetic parameters, p. 10.



F4. Hole 1202B magnetic parameters, p. 11.



## ROCK MAGNETIC RESULTS

### Hole 1202A

The MS is generally  $\sim 20 \times 10^{-5}$  SI in the upper 11.5 m and lowermost 1.5 m of the sequence (Fig. F3). In the interval between 111.5 and 118 mbsf, the values are slightly lower, in the range of  $15 \times 10^{-5}$  SI.

The NRM intensity is  $< 1 \times 10^{-2}$  A/m except for two spikes at 100.9 and 102.3 mbsf. At the same depths, high values of MS and ARM intensity are observed (Fig. F3). The features of the NRM intensity are mirrored in the ARM intensity and ARM/k ratio, with higher values in the upper 3 m of the core and in the shorter interval at 108–109.5 mbsf. The magnetic hardness ( $ARM_{30 \text{ mT}}/ARM_{0 \text{ mT}}$ ) is relatively constant from the bottom of the cored section up to 103 mbsf, at which point it increases slightly, similar to the other parameters. The Day plot (Day et al., 1977) (Fig. F5) shows that the grain size of the magnetic carriers is variable, but falls within the pseudo-single-domain field for magnetite.

### Hole 1202B

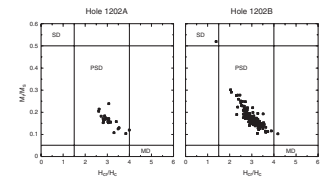
The NRM intensity is  $7.4 \times 10^{-3}$  A/m on average, with highest values in the intervals between 0 and 40 and between 84 and 110 rmbfsf (Fig. F4). The uppermost interval is characterized by a distinct intensity peak with values as high as 0.024 A/m.

The typical MS value is  $\sim 20 \times 10^{-5}$  SI, but many  $> 200 \times 10^{-5}$  SI are present, especially in the depth intervals between 80 and 94 and between 101 and 110 rmbfsf. In these intervals, the spikes in MS often correspond to spikes in the NRM and ARM intensity. Although the MS signal is rather noisy, a trend is clearly discernable. After a slight down-core decrease at the uppermost part in the most recent sediment, the MS shows a trend characterized by two peaks at  $\sim 30$  and 68 rmbfsf. A correspondence exists between the MS and NRM intensity in those intervals in which the latter is high, but the MS in the rest of the core is characterized by significant variability. The ARM intensity is similar to the NRM intensity except in the interval between 69.4 and 86.5 rmbfsf, where the ARM intensity tends to increase.

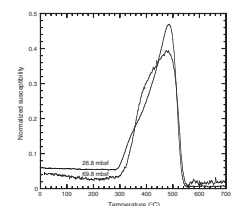
The parameters ARM/k and magnetic hardness ( $ARM_{30 \text{ mT}}/ARM_{0 \text{ mT}}$ ) are commonly used in environmental magnetism. They are sensitive to the magnetic grain size and coercive force. In this case, they mirror the ARM intensity, with the highest values in the intervals at 0–40 and 69.4–110 rmbfsf. As in Hole 1202A, the hysteresis parameters suggest that the magnetic carriers fall within the range of pseudo-single-domain magnetite grains (Fig. F5).

The thermoremanence investigations indicate that the dependence of the MS with temperature is similar throughout the sequence (Fig. F6). The heating curves show a strong increase in MS after 280°–300°C because of chemical alterations during heating. A prominent peak appears at  $\sim 490^\circ\text{C}$  and is followed by a sharp drop in the MS, indicating a Curie temperature ( $T_c$ ) of  $\sim 540^\circ\text{C}$ . This is 40°C lower than the Curie temperature of pure magnetite and is indicative of a low-titanium magnetite generated during the heating process.

F5. Hysteresis parameters, p. 12.



F6. Hole 1202B thermomagnetic behavior, p. 13



## ACKNOWLEDGMENTS

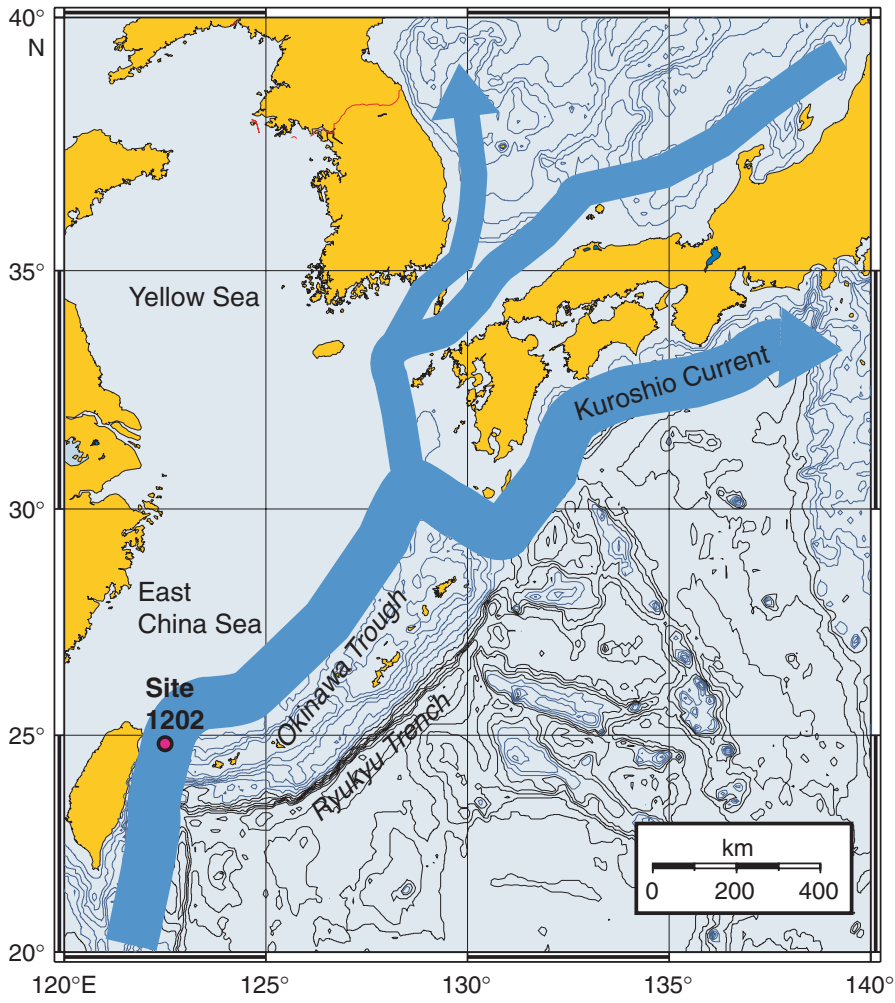
We thank members of the ODP Leg 195 shipboard scientific party for numerous discussions and acknowledge the support and cooperation of the ODP personnel, Captain T. Hardy, and the crew of the *JOIDES Resolution*. We are grateful to Stefanie Brachfeld for her helpful and critical comments on the original manuscript. This research used samples and/or data provided by the Ocean Drilling Program (ODP). ODP is sponsored by the U.S. National Science Foundation (NSF) and participating countries under management of Joint Oceanographic Institutions (JOI), Inc. We gratefully acknowledge JOI for a JOI/USSAC (U.S. Science Advisory Committee) grant to C. Richter that provided funding for this work.

## REFERENCES

- Berggren, W.A., Kent, D.V., Swisher, C.C., III, and Aubry, M.-P., 1995. A revised Cenozoic geochronology and chronostratigraphy. In Berggren, W.A., Kent, D.V., Aubry, M.-P., and Hardenbol, J. (Eds.), *Geochronology, Time Scales and Global Stratigraphic Correlation*. Spec. Publ.—SEPM (Soc. Sediment. Geol.), 54:129–212.
- Boggs, S., Jr., Wang, W.C., Lewis, F.S., and Chen, J.-C., 1979. Sediment properties and water characteristics of the Taiwan shelf and slope. *Acta Oceanogr. Taiwanica*, 10:10–49.
- Day, R., Fuller, M., and Schmidt, V.A., 1977. Hysteresis properties of titanomagnetites: grain-size and compositional dependence. *Phys. Earth Planet. Inter.*, 13:260–267.
- Hrouda, F., 1994. A technique for the measurement of thermal changes of magnetic susceptibility of weakly magnetic rocks by the CS-2 apparatus and KLY-2 Kappa-bridge. *Geophys. J. Int.*, 118:604–612.
- Jian, Z., Wang, P., Saito, Y., Wang, J., Pflaumann, U., Oba, T., and Cheng, X., 2000. Holocene variability of the Kuroshio Current in the Okinawa Trough, northwestern Pacific Ocean. *Earth Planet. Sci. Lett.*, 184:305–319.
- Lin, F.-T., and Chen, J.-C., 1983. Textural and mineralogical studies of sediments from the southern Okinawa Trough. *Acta Oceanogr. Taiwanica*, 14:26–41.
- Moran, K., 1997. Elastic property corrections applied to Leg 154 sediment, Ceara Rise. In Shackleton, N.J., Curry, W.B., Richter, C., and Bralower, T.J. (Eds.), *Proc. ODP, Sci. Results*, 154: College Station, TX (Ocean Drilling Program), 151–155.
- Sagnotti, L., and Winkler, A., 1999. Rock magnetism and palaeomagnetism of greigite-bearing mudstones in the Italian peninsula. *Earth Planet. Sci. Lett.*, 165:67–80.
- Sawada, K., and Handa, N., 1998. Variability of the path of the Kuroshio ocean current over the past 25,000 years. *Nature*, 392:592–595.
- Shipboard Scientific Party, 2001. Site 1166. In O'Brien, P.E., Cooper, A.K., Richter, C., et al., *Proc. ODP, Init. Repts.*, 188, 1–110 [CD\_ROM]. Available from: Ocean Drilling Program, Texas A&M University, College Station TX 77845-9547, USA.
- Shipboard Scientific Party, 2002. Site 1202. In Salisbury, M.H., Shinohara, M., Richter, C., et al., *Proc. ODP, Init. Repts.*, 195, 1–46 [CD-ROM]. Available from: Ocean Drilling Program, Texas A&M University, College Station TX 77845-9547, USA.
- Sibuet, J.-C., Deffontaines, B., Hsu, S.-K., Thareau, N., Formal, J.-P., Liu, C.-S., and the ACT party, 1998. Okinawa Trough backarc basin: early tectonic and magmatic evolution. *J. Geophys. Res.*, 103:30245–30267.
- Snowball, I.F., 1997. Gyroremanent magnetization and the magnetic properties of greigite-bearing clays in southern Sweden. *Geophys. J. Int.*, 129:624–636.
- Ujiié, H., Tanaka, Y., and Ono, T., 1991. Late Quaternary paleoceanographic record from the middle Ryukyu Trench slope, northwest Pacific. *Mar. Micropaleontol.*, 18:115–128.
- Ujiié, H., and Ujiié, Y., 1999. Late Quaternary course changes of the Kuroshio Current in the Ryukyu arc region, northwestern Pacific Ocean. *Mar. Micropaleontol.*, 37:23–40.
- Verosub, K.L., 1998. Faster is better. *Science*, 281:1297–1298.
- Wang, K.L., Chung, S.-L., Chen, C.-H., Shinjo, R., Yang, T.-F., and Chen, C.-H., 1999. Post-collisional magmatism around northern Taiwan and its relation with opening of the Okinawa Trough. *Tectonophysics*, 308:363–376.
- Weeks, R.J., Laj, C., Endignoux, L., Fuller, M.D., Roberts, A.P., Manganne, R., Blanchard, E., and Goree, W., 1993. Improvements in long-core measurement techniques: applications in palaeomagnetism and palaeoceanography. *Geophys. J. Int.*, 114:651–662.

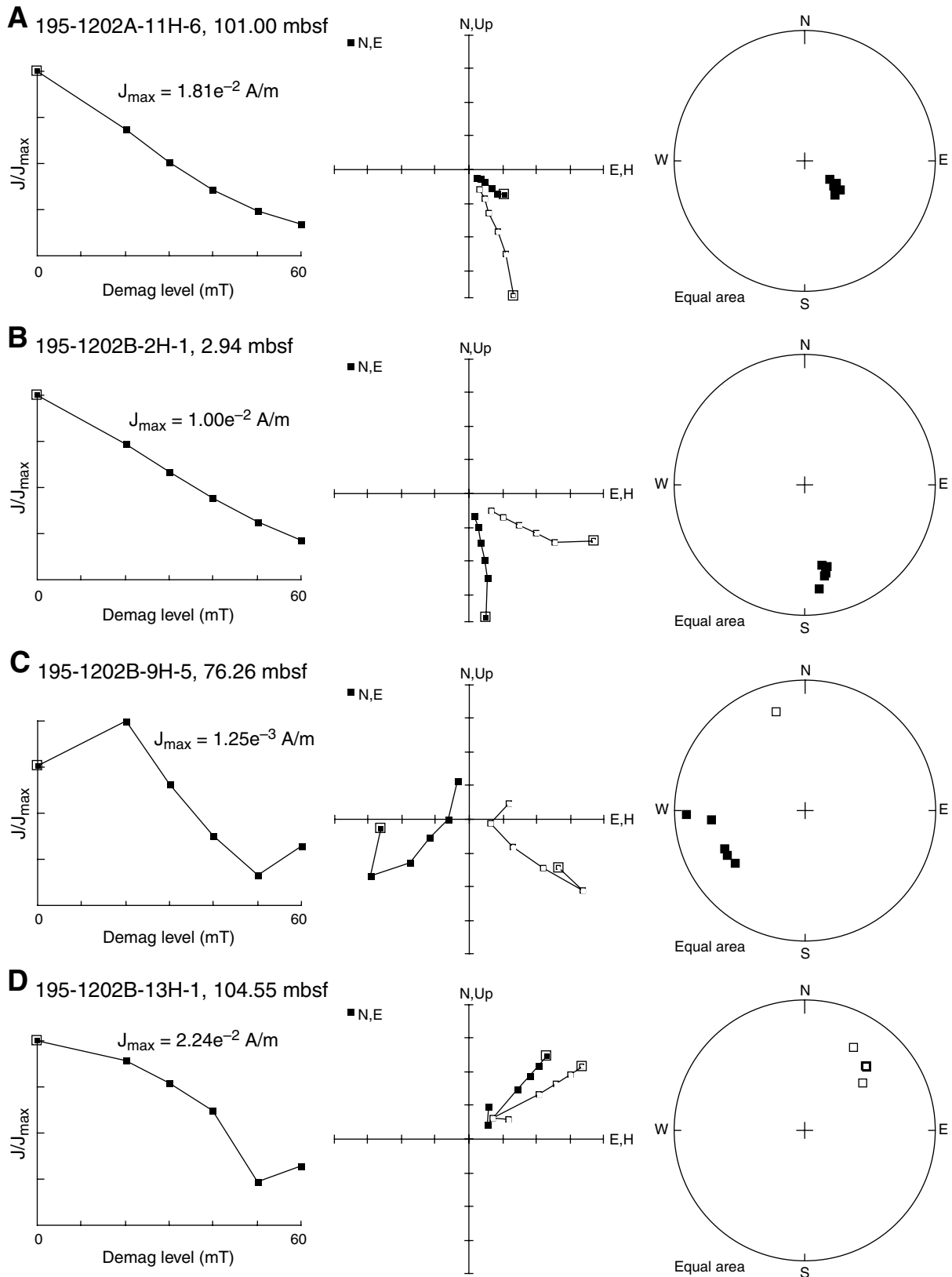


Figure F1. Location of Site 1202 in the Southern Okinawa Trough and path of the Kuroshio Current.





**Figure F2.** Vector component diagrams with normalized intensity decay plots and stereographic projections of alternating-field (AF) demagnetization behavior for four representative samples from Holes 1202A and 1202B. Open (closed) symbols represent projections on the vertical (horizontal) plane. **A.** Section 195-1202A-11H-6. **B.** Section 195-1202B-2H-1. **C.** Section 195-1202B-9H-5 **D.** Section 195-1202B-13H-1.



**Figure F3.** Downcore variations of magnetic parameters (NRM intensity and inclination, magnetic susceptibility, and ARM intensity), relative magnetic grain-size proxy (ARM/k), and magnetic hardness ( $ARM_{30\text{ mT}}/ARM_{0\text{ mT}}$ ) determined in Hole 1202A. NRM = natural remanent magnetization, ARM = anhysteretic remanent magnetization.

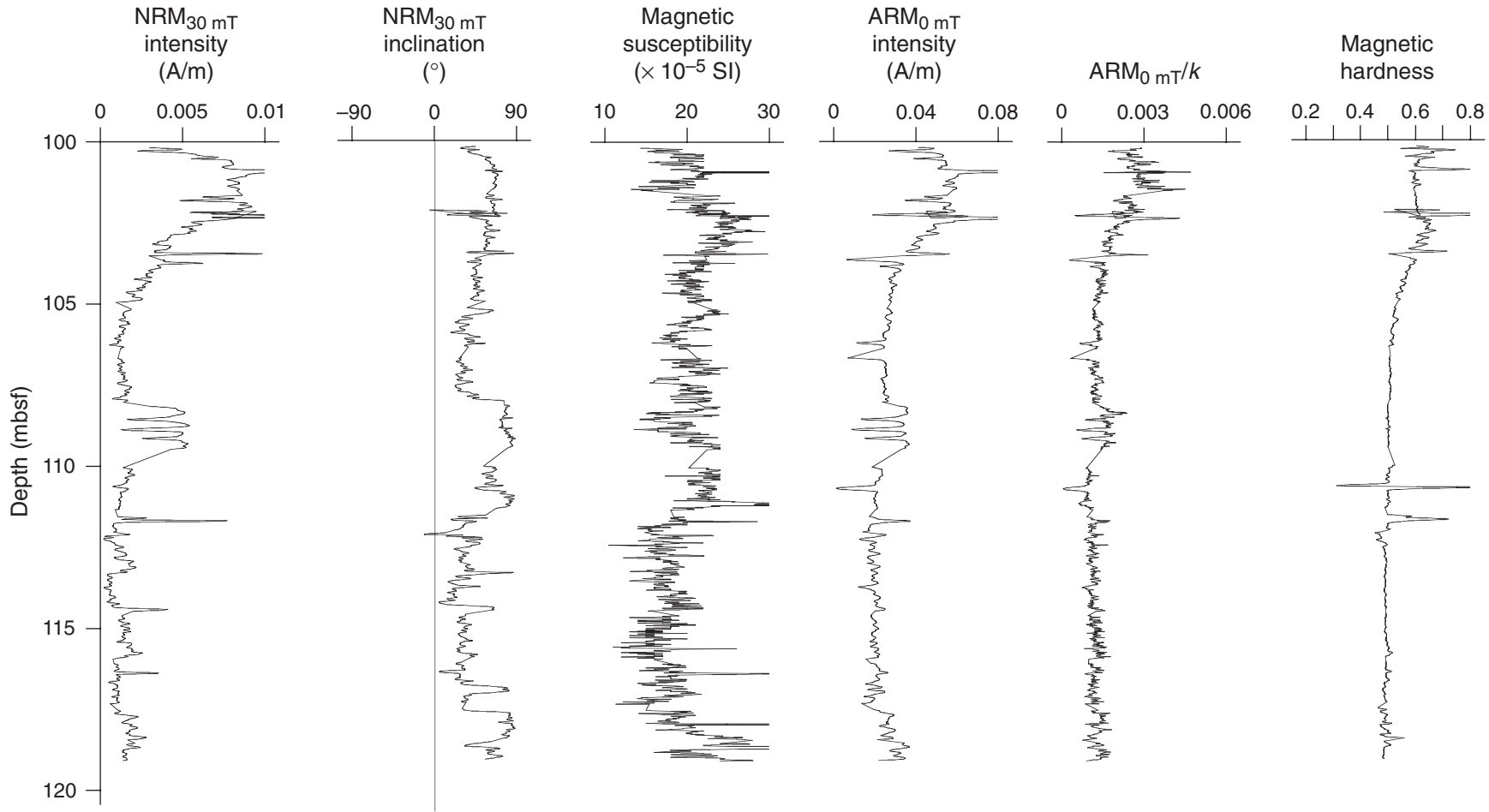


**Figure F4.** Downcore variations of magnetic parameters (NRM intensity and inclination, magnetic susceptibility, and ARM intensity), relative magnetic grain-size proxy (ARM/k), and magnetic hardness ( $ARM_{30\text{ mT}}/ARM_{0\text{ mT}}$ ) determined in Hole 1202B. NRM = natural remanent magnetization, ARM = anhysteretic remanent magnetization.

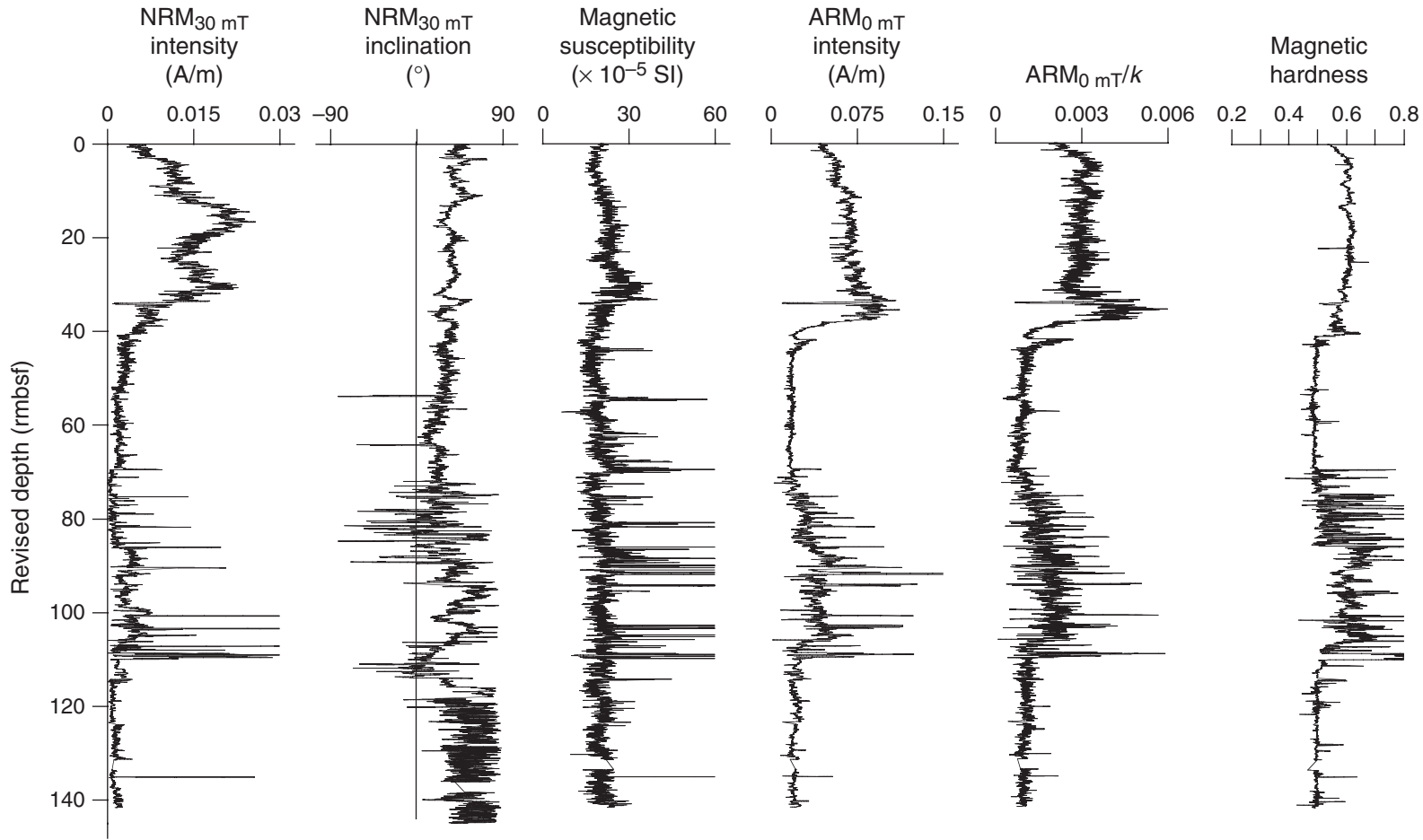


**Figure F5.** Hysteresis parameters displayed in a Day plot (Day, 1977) from Hole 1202A (diagram on left) and Hole 1202B (diagram on right). SD = single domain, PSD = pseudo-single domain, MD = multiple domain.

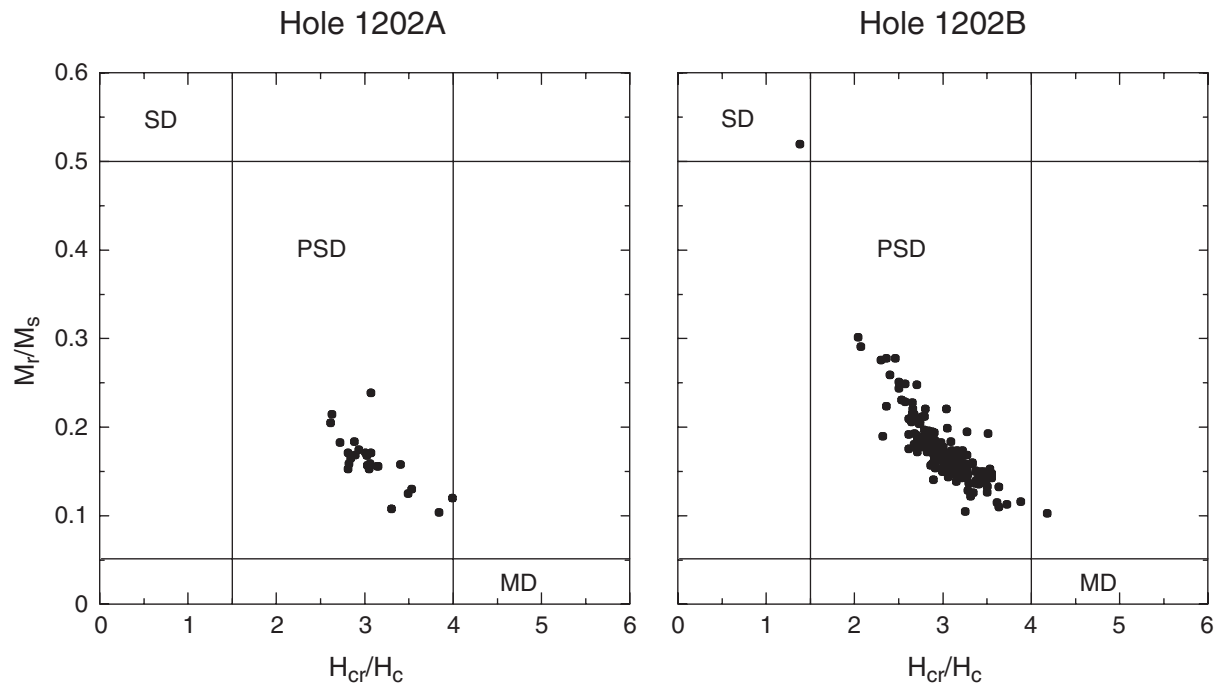
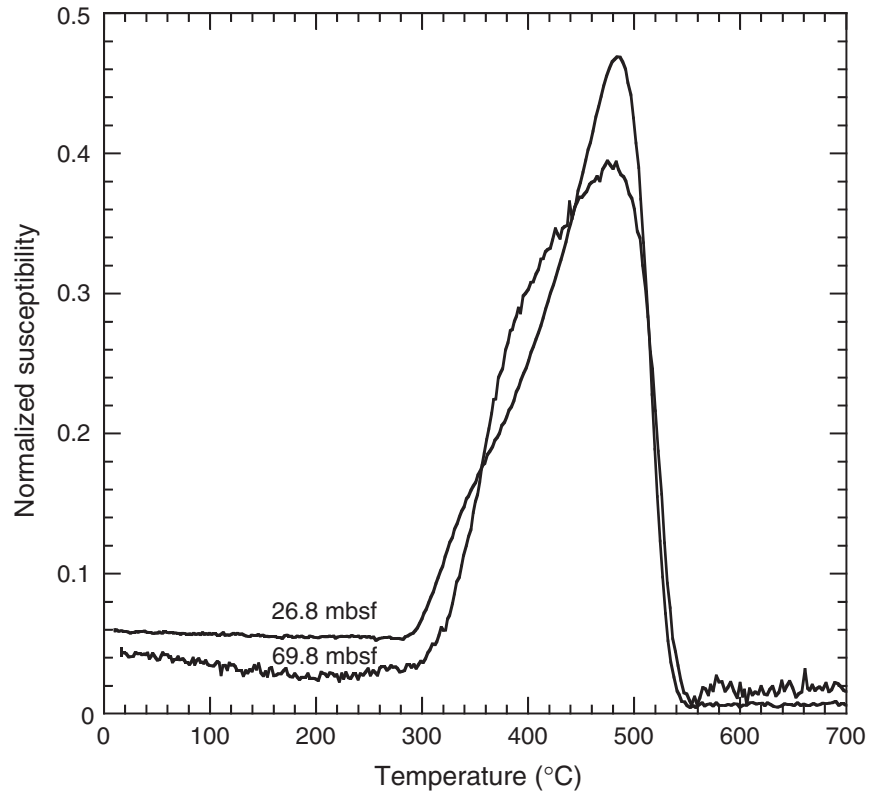


Figure F6. Thermomagnetic behavior of two samples from Hole 1202B (heating curves only) display a strong increase in susceptibility between 300° and 500°C and a Curie temperature of 540°C.



**Table T1.** The revised depth model accounts for core expansion.

Core	Offset (m)	Top of Core	
		Depth (mbsf)	Depth (rmbfsf)
195-1202B-			
1H	0	0	0
2H	0	2.9	2.9
3H	0.207	12.4	12.607
4H	0.225	21.9	22.125
5H	0.541	31.4	31.941
6H	0.837	40.9	41.737
7H	1.605	50.4	52.005
8H	1.931	59.9	61.831
9H	2.145	69.4	71.545
10H	2.461	78.9	81.361
11H	2.461	88.4	90.861
12H	2.578	97.9	100.478
13H	2.578	104.2	106.778
14X	2.578	111.6	114.178
15X	2.578	121.2	123.778
16X	2.578	130.9	133.478

Note: A constant offset is added to each core to avoid overlapping measurements. Conversion between the two depth scales requires addition (subtraction) of the offset constant to (from) the mbsf (rmbfsf) scale.